Tracking the paths for the sucrose transformations over bifunctional Ru-POM/AC catalysts

N. García-Bosch[a,b]*, Catherine Especel[c], A. Guerrero Ruiz[a]*, I. Rodríguez-Ramos[b]*

[a]*Dpto. Química Inorgánica y Técnica, Facultad de Ciencias UNED, 28040 Madrid, Spain*

[b]*Instituto de Catálisis y Petroleoquímica, CSIC, Cantoblanco, 28049 Madrid, Spain*

[c]*Université de Poitiers, CNRS UMR 7285 IC2MP, Institut de Chimie des Milieux et des Matériaux de Poitiers, 86073 Poitiers, France*

*Corresponding authors: ngarcia@ccia.uned.es, aguerrero@ccia.uned.es, irodriguez@icp.csic.es

ABSTRACT

The possible pathways of sugars transformation into 1,2-propanediol (PDO) have been studied, using new bifunctional catalysts for this catalytic multistep reaction. The catalysts are based on an acidic active phase (polyoxometalates, POMs) and a metallic function (Ru nanoparticles) supported over activated carbon (AC, S_{BET} = 1190 m^2/g). This support was loaded with 15wt% of polyoxometalate, either phosphotungstic acid (TPA) or tungstosilicic acid (STA), while the amount of loaded ruthenium was close to 2wt%. The catalytic materials were characterized by X-ray diffraction and electron microscopy techniques (SEM and TEM), while the surface active sites were evaluated using model reaction tests: cyclohexane dehydrogenation for metallic surface sites and isomerization of 3,3-dimethyl-1-butene for acid sites. For different sugars (sucrose, pentoses or hexoses) hydrogenation/hydrogenolysis using these catalysts in batch reactor was studied. The higher PDO selectivity was obtained in ethanol:water media and this study aims to establish the possible ways that sugars follow to achieve this transformation. The best catalytic material, 2%Ru-15%STA supported on AC, yields up to 50% of PDO selectivity when fructose is used as reactant, under moderate reaction conditions (413 K and 30 bar H$_2$).

Keywords: activated carbon; polyoxometalates; ruthenium; fructose conversion; 1,2-propanediol

1. Introduction

Over last few years, one of the most attention focuses is the heterogeneous catalysis and its application in the synthesis of platform molecules from biomass. Taking into account the depletion of fossil resources, the necessity to find a new renewable resource becomes evident, for that the development of biomass transformation reactions is increasing exponentially [1, 2, 3]. Thus, new catalytic processes have been vigorously studied worldwide in attempt to transform biomass into valuable chemicals named platform molecules. One of the important and used macromolecules to obtain some petroleum derived compounds are the cellulose or hemicellulose, which also can be converted into hexose and pentose, through easy hydrolysis reactions catalysed by acids, where these macromolecules are cracked into some of its monomers (carbohydrates such as glucose or xilose) [4, 5, 6, 7]. While fructose is easily derived from glucose or xylose, there are other sources to obtain the saccharides, for instance sucrose is produced directly from sugar cane [8, 9].Then the transformations of these platform molecules derived from biomass is one way to achieve compounds able to replace the petroleum derivatives as primary source [10, 11]. 1,2-propanediol (PDO) is a chemical compound with high added value in bio-oil industry, and for that recently, studies about propylene glycol or PDO synthesis have been reported [12, 13, 14]. Particularly hydrogenation and/or hydrogenolysis reactions of sugars, as sustainable biomass resources, can produce various polyols (sorbitol, glycerol, PDO) using metallic catalysts [15,16,17]. Recently Almeida et al. [18] studied the one-pot conversion of cellobiose into sorbitol and reported that the bifunctionality of catalysts with acid and metallic contributions plays a major role in this reaction.

PDO synthesis from derived biomass compounds, such as cellulose and glucose, may be achieved using bifunctional catalysts (metallic-acidic functionalization) because this reaction involves two or three different catalytic transformations: firstly, starting from cellulose, a hydrolysis (acid catalysis) is needed to obtain hexoses and pentoses, and later these compounds have to be hydrogenated (catalysed by metals) and suffer hydrogenolysis (favoured by metals and/or by acids catalysts) to yield PDO. It is for this reason that in literature it is possible to see some articles where the catalysts studied for hydrogenation/hydrogenolysis have these two functionalities [12,19], for instance in some cases the supports display the acid contribution (zeolites and acidic oxides) [14,20]. In this line Hirano et al. [21] compared a variety of catalytic materials composed by different metals (Rh, Pd, Pt and Ru) supported over carbon combined with different acids, normally metallic oxides. They reported a 38% maximum yield of PDO obtained when the zinc oxide combined with Ru/C was tried at 453 K. With the objective to improve the results described, other solid acids such as polyoxometalates should be evaluated. Due to the high acidity of polyoxometalates (POMs) in comparison with zeolites, acidic resins and inorganic acids (H_2SO_4), these materials should be a good option to improve these catalytic results [22]. Consequently, some authors have already studied the cellulose transformation to sugars alcohols using polyoxometalates as acidic phase [7,13,23]. However, there are fewer reported studies about transformation of sucrose, glucose and fructose using POMs such as supported acid phase in catalyst surface. Although, as it has been mentioned in ref [19], the WO_x species in metal-acid bifunctional $Cu-WO_x/Al_2O_3$ catalysts are found to be responsible of the increment of PDO selectivity in the hydrogenolysis of glucose. Therefore, we could assume that the PDO selectivities and yields will be improved using POMs, such

as phosphotungstic acid (TPA, $H_3PW_{12}O_{40}$) and silicotungstic acid (STA, $H_4[W_{12}SiO_{40}]$), due to the Bronsted acidity of WO_x groups.

On the other hand, activated carbon (AC) is one potential POM support to be used in this type of catalytic reactions [24], though there are other materials such as zeolites, silica, alumina or metal oxides (Fe_2O_3, ZnO, ZrO_2) which could also be chosen [25, 26]. Normally, the characteristics of active species (POMs and metal) determine the support properties needed to optimize the catalytic process, mainly the catalytic selectivity achieved with the bifunctional material. Then, taking into account that the POMs have high acidity, the support should be an inert material to favour weak interactions with nanocristallites of POMs and maximize strong interactions among the two supported active phases (metallic nanoparticles and POMs crystallites). Carbonaceous materials usually have a low reactivity with the supported species, particularly the activated carbon is a good option because it presents a minor interaction with this type of superacids compared, for example, to the graphitic surfaces [27]. Therefore, due to the low reactivity of AC and other favourable properties such as pH stability and high surface area, which favours high dispersion of active phases, AC was chosen as support in some reported articles [28, 29], and also to synthetize the new catalytic materials used in the present study.

Scheme 1 shows the possible pathways that sugars can follow according to the active sites exposed over the catalyst surfaces. Firstly, when the catalytic material exhibits only an acidic contribution, the sucrose is hydrolysed to glucose and fructose (step 1) or to its ethylated molecules (E-glucose or E-fructose) (step 2), due to the presence of ethanol as solvent in the reaction media. Subsequently, they can suffer dehydration reactions, yielding 5-hydroxymethyl furfural (5-HMF), following the step 3 of Scheme 1. As it is known the dissociation of H_2 is catalysed by metals, so metallic surface sites

are required for the hexoses hydrogenation. Therefore with this metallic contribution, the sucrose is also hydrolyzed to hexoses or to E-hexoses, but now producing hydrogenation reactions to sorbitol or mannitol (paths 4 and 5), which can also suffer an isomerization themselves. The next step, the hydrogenolysis of fructose/E-fructose or sorbitol/mannitol into glycerol, follows the steps 6 and 7 of Scheme 1 and later this product transforms into 1,2-PDO through step 8. But, PDO can also be obtained by a direct route from fructose (step 9), as it has been reported by Zang and coworkers [19], with catalysts containing double functionality (acid and metallic) as well. Then, in these last steps of the catalytic scheme an adequate ratio of acid/metallic sites over catalyst surface can be crucial for achieving better selectivities for fructose hydrogenolysis compounds, in particular for obtaining propylene glycol or 1,2-PDO [19]. In general these reaction paths are in good agreement with the proposed by P.A. Lazaridis et al [17], reported in a study of cellulose hydrolytic hydrogenation over Pt and Ru catalysts supported on acidic porous carbons.
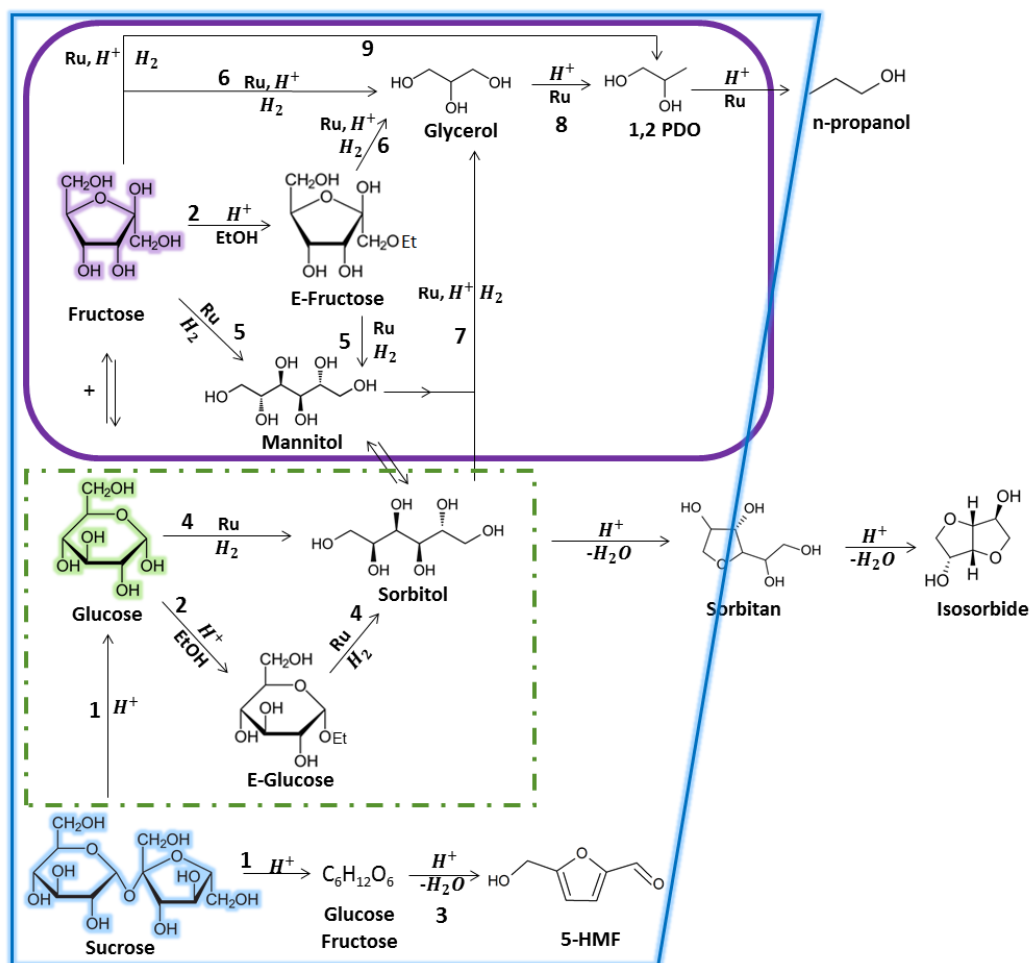
Scheme 1: Possible routes of sugars (sucrose, glucose and fructose) transformation into hydrogenation/hydrogenolysis products such as glycerol and PDO (using or not ethanol as solvent).

Then, herein we report a new sequence of bifunctional catalysts based on POMs and Ru nanoparticles supported over activated carbon (AC) to be used in the catalytic sugar transformation. Also the possible pathways of the reaction are discussed. Due to the high solubility of POMs in water versus its lower solubility into ethanol [27], the solvent used for this work has been a mixture of ethanol:water (9:1). On the other hand, the low thermal stability of sugars, due to its high content of hydroxyl groups, makes the reaction temperature another point to take into account in this chemical

transformation, which should be as low as possible. Therefore, in this work the reaction conditions were fixed at 413 K of reaction temperature and 30 bar of H_2 atmosphere because using higher temperatures the sugars suffer thermal degradations.

2. Experimental

2.1 Catalysts preparation

The catalysts were synthetized using a high purity activated carbon (AC) as support, produced from olive stones by Oleicola el Tejar, Córdoba Spain. This carbonaceous material was sieved to 1.25–0.8 mm of grain sizes and its BET area is 1190 $m^2 \cdot g^{-1}$ [27]. This support is treated with hydrochloric acid solution 10% (v/v) at 373 K for 24 h, in order to remove residual inorganic components, and subsequently filtered and washed with distilled water until complete removal of detectable Cl^- ions. The synthesis method of catalysts consists in simple or successive incipient impregnation with solutions in ethanol:H_2O (1:1), where firstly POM and secondly Ru precursors are deposited, in the case of bifunctional materials. Used POMs were STA ($H_4[W_{12}SiO_{40}]$) or TPA ($H_3PW_{12}O_{40}$) and the Ru precursor was ruthenium chloride ($RuCl_3 \cdot H_2O$). All these reactants are of high purity degree and were provided by Sigma Aldrich. Once the activated carbon support is impregnated with POMs and/or Ru solutions, the catalysts were dried/stabilized at 373 K in an air oven during 16 h and stored in dry atmospheres [13]. The amounts of POMs and Ru loaded were close to 15 wt% and 2 wt%, respectively. Prior to the catalytic tests the materials with metallic components (Ru) were reduced at 623 K for 1 h under H_2 flow (60 $cm^3 \cdot min^{-1}$). Subsequent to the reduction treatment, the stability of POMs and carbon supports were tested and under these conditions of reduction, both materials (POMs and supports) are stable. As a list of the prepared samples we have: STA-AC, Ru-AC, Ru-STA-AC and Ru-TPA-AC.

2.2 Catalysts characterization

The structural properties of the synthetized materials were studied by X-ray diffraction (XRD). The patterns were obtained on a Polycrystal X'Pert Pro PANalytical instrument, with Ni-filtered CuKα X-rays (λ = 1.54 Å). Bragg's angles between 5 and 95 were scanned at a rate of 0.058 °/s.

Transmission electron microscopy (TEM) using a JEOL 2100 F field emission gun operated at 200 kV and EDX mode were used to study the ruthenium particle sizes, dispersion and atomic arrangement. The TEM analyses were performed on the samples after reduction at 623 K during 1 h or after reaction, after grinding and suspension in ethanol by ultrasonic treatment. A drop of this suspension was placed on a carbon-coated copper grid of 200 mesh (Aname). Average particle size (d_{TEM}) was calculated based on a minimum of 200 particles using $d_{TEM} = \sum n_i d_i^3 / \sum n_i d_i^2$ where n_i is the number of particles with d_i diameter. In order to gain information about the morphological characteristics of the polyoxometalates supported over activated carbon support, the catalysts were studied also by scanning electron microscopy (SEM). The equipment employed was Hitachi TM-1000. Energy dispersive X-ray spectroscopy (EDX) mode was used to determine the presence of metals (Si or P and W).

Characterization of acidity and metallic contributions over carbon supports were measured through two model test reactions. Isomerization of 3,3-dimethyl-1-butene was tested using a fixed-bed tubular glass reactor working at atmospheric pressure. The 3,3-dimethyl-1-butene was fed into the reactor by bubbling a flow of nitrogen (30 cm^3 min^{-1}) through a saturator-condenser into ice bath. In a typical experiment, an aliquot of sample of 100 mg (sized at 0.35-0.5 mm) was pre-treated inside the reactor at 623 K

during 1 h under continuous flow of H_2 (60 cm^3 min^{-1}). After cooling at 423 K in inert flow, the reaction was started at this temperature by feeding the 3,3-dimethyl-1-butene mixture (vaporized reactant with a partial pressure of 20 kPa in N_2 gas). The reaction products were analyzed by gas chromatography (AlphaMos PR2100) with a flame ionization detector (FID) and a RTx-1 (Restek) column (105 m $\times$ 0.53 mm $\times$ 3.00 μm) [30]. The initial catalytic activity has been calculated using the mathematical equation presented below:

$$A\left(\frac{\text{mmol}}{\text{h} \, x \, g_{catalyst}}\right) = \frac{Conv_i \, (\%) x \, F_{reactant}}{100 \, x \, g_{catalyst}}$$

where $F_{reactant}$ is the reactant flow expressed as mmol/h and $Conv_i$ is the initial conversion calculated by using the interception of obtained line of fit of 3,3-dimethyl-1-butene conversion values. The test reaction used for metallic centers characterization was dehydrogenation of cyclohexane to benzene. The dehydrogenation reaction was carried out in a fixed-bed glass reactor under atmospheric pressure and with 70 mg of catalyst. The catalyst was heated to 623 K under continuous H_2 flux (60 cm^3 min^{-1}) during 1 h, then the temperature was cooled down to 543 K for starting the reaction using higher H_2 flux (100 cm^3 min^{-1}) and a continuous flow of liquid reactant (0.03 cm^3 min^{-1}) injected upstream of the reactor. The products were analyzed by gas chromatography (Varian 3400X with FID detector), using an automatic injection valve ensuring sampling at regular time intervals [31]. In this second case, a similar calculus to obtain the initial activity was used:

$$A\left(\frac{\text{mol}}{\text{h} \, x \, g_{metal}}\right) = \frac{Conv_i \, (\%) x \, F_{reactant}}{100 \, x \, g_{metal}}$$

but in this case the reactant flow is expressed as mol/h and the activity per gram of active phase (metal). The $Conv_i$ has been calculated using the same strategy than the isomerization test.

The possible leaching of POM elements (i.e. tungsten and silicon or phosphorus) or ruthenium metal was verified by analyzing the final reaction mixture by Inductively Coupled Plasma mass spectrometry (ICP-OES Optima 3300 DV Perkin Elmer). Determining tungsten or ruthenium concentration made possible to know the percentage (%) of each metal dissolved into the reaction medium.

2.3 Catalytic reaction

The catalytic properties (activity and selectivity) of carbohydrates transformation in hydrogenation/hydrogenolysis reactions were studied using a 100 ml Teflon-lined stainless steel autoclave (Parr 4072, Parr Instrument Co.). These typical catalytic reactions were carried out at 413 K and under 30 bar of H_2 using 90 ml of a mixture of ethanol/water (9:1) as solvent, and 100 mg of both reactant and catalyst. All this mixture was added into the reactor that was flushed with He, to exclude air, and later with H_2 at 10 bar. Then, the batch reactor was heated to reaction temperature and also stirred at 500 rpm. When the reaction temperature was reached after 30 min, the pressure is adjusted to 30 bar of H_2, the reaction time was set to zero and data were recorded thereafter. Similar masses of catalysts were studied in all catalytic tests and the liquid aliquots were extracted at the same periodic times, in order to compare all products evolutions. Finally, the liquid samples were filtered (0.2 μm-PTFE membrane) and analysed by HPLC with an Agilent system equipped with a Hi-plex H column, eluting with an aqueous solution of 0.005 M sulphuric acid (rate 0.6 mL/min) as mobile phase and by using an refractive index detector. Standard solutions covering the concentration range of the samples were used to obtain the calibration curves for calculating concentration of interest compounds. After 5 h reaction time, the results

such as conversions and yields were calculated as it has been previously reported in literature [27].

The mathematic equations employed to calculate conversion is:

$$Conv\ (\%) = \frac{C_{sugar}^0 - C_{sugar}^i}{C_{sugar}^0} \ x\ 100$$

Where C_{sugar}^0 is the reactant concentration and C_{sugar}^i the concentration of unreacted reactant in i time. The yields were calculated by the next formula:

$$Y_i(\%) = \frac{n \cdot X_{product}^i}{X_{sugar}^0} \ x\ 100$$

Where $X_{product}^i$ refers to moles number of studied product and corrected by the stoichiometry factor of the reaction (n), while X_{sugar}^0 correspond to initial moles number of reactant. Finally, the carbon balances are also calculated where the employed equation has been:

$$C_B(\%) = \frac{\sum n \cdot X_{reac/prod}^i}{X_{sugar}^0}$$

This value is defined as quotient between summation of all compounds moles (reactant + products) in i time and initial reactant number of moles (X_{sugar}^0).

3. Results and discussion

3.1 Catalysts characterization

X-ray diffraction (XRD) patterns are showed in Figure 1, where bare AC support and the catalysts (reduced under hydrogen flow at 623 K) are compared. All diffractograms

exhibit the same two peaks around 26 and 45°, corresponding to diffraction of the 002 and 100/101 planes, respectively, observed on activated carbon (AC). So, it is assumed that the majority of metallic nanoparticles and POMs crystallites are in the nanometric scale, with dimensions lower than 5 nm and/or poor crystallinity. Therefore the characteristic peaks of metallic ruthenium or POMs are not detectable [27].
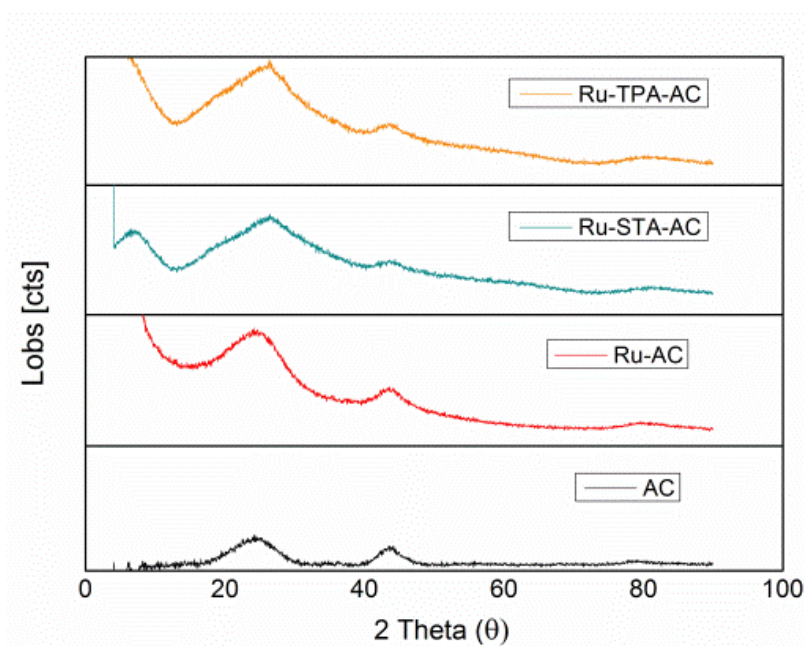

Figure 1: X-ray diffraction of bulk support (AC) and bifunctional, monofunctional catalysts.

To corroborate this preliminary conclusion from the XRD profiles, TEM and SEM characterizations have been used in order to provide direct information about metallic nanoparticles sizes. Figure 2 shows a representative TEM image of the bifunctional catalysts (Ru-STA-AC given as example) and the histogram of nanoparticles distribution sizes. For both bifunctional and monofunctional catalysts, a quasi-symmetric distribution of sizes is observed, with an average size of ruthenium

nanoparticles of 1.3 nm, in the case of bifunctional solids. However the average diameter of the Ru particles, in the reduced Ru-CA sample, is rather higher (in the range of 2.5-5.5 nm). In fact this finding could be considered as a probe of the existence of specific interactions between the polyoxometalates and the Ru precursor during the catalyst preparations. So we can confirm that the Ru nanoparticles are nanometric. Contrarily the POM crystallites sizes can't be observed using TEM due to the low electron density of metal oxides, impeding a good contrast of POM with carbon support. However, the presence of acid active phase (POM) onto the carbon support can be confirmed due to signals of tungsten atoms detected by EDX analysis (Figure 2c). So, combining the results obtained by these two characterization techniques, we conclude that carbon support is decorated with POM crystallites and ruthenium particles of nanometric size.
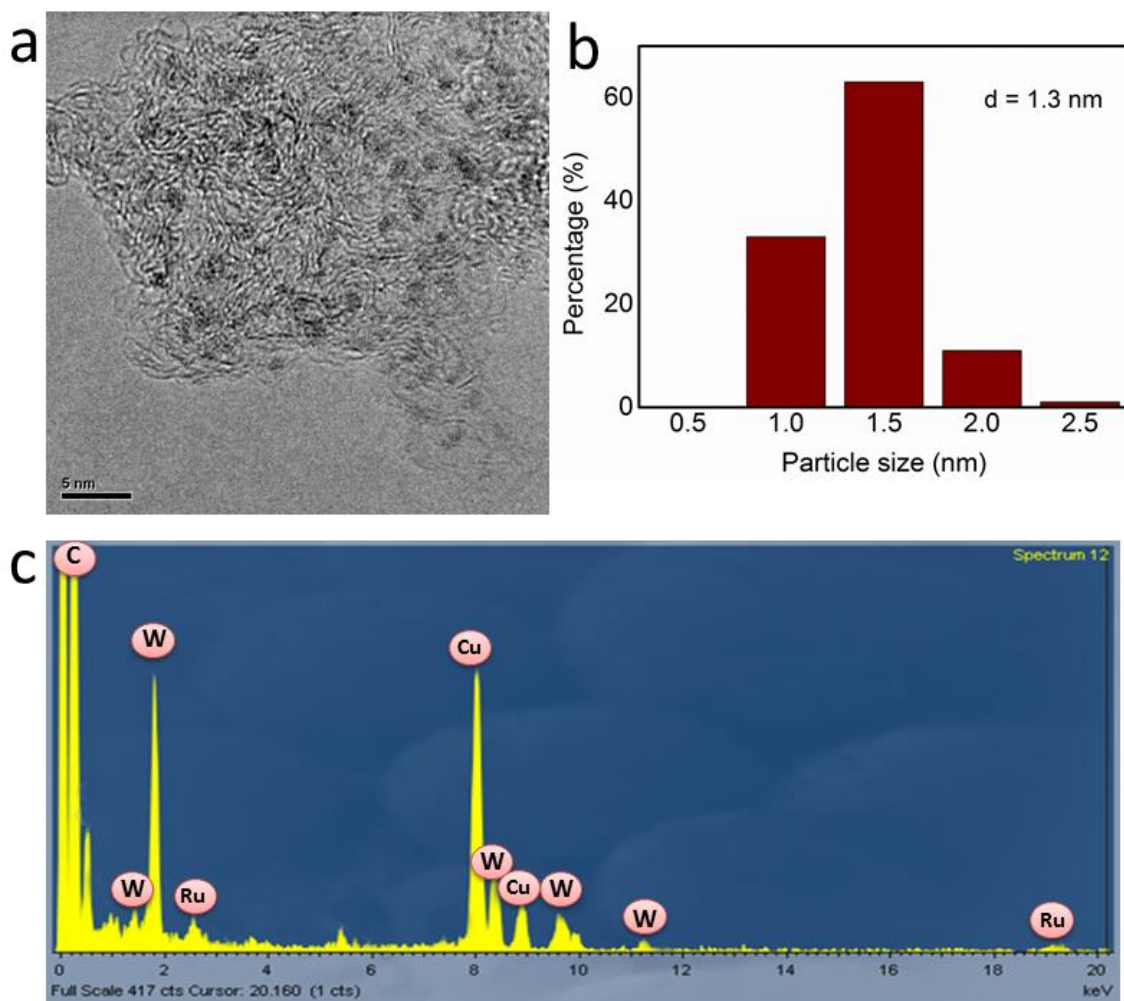
Figure 2: (a) TEM images of fresh Ru-STA-AC catalyst previously reduced under hydrogen flow at 623 K, (b) histogram of Ru nanoparticle sizes and (c) Energy dispersive X-ray analysis of the samples.

Two representative SEM images are presented in Figure 3, where the fresh Ru-STA-AC sample and the same material after reaction are compared. Thereby, differences in morphological characteristics are observed between the fresh and used sample, since the first one presents big POM crystallites (Fig. 3a) which disappear in the second image (Fig. 3b). This fact means that there are some big amorphous particles over the fresh

catalyst detectable by SEM, but they disappear when this material has been used in reaction. Provably these big POM crystallites are dissolved in reaction media [27]. Therefore, some leaching of POM seems to occur, which will be studied later.
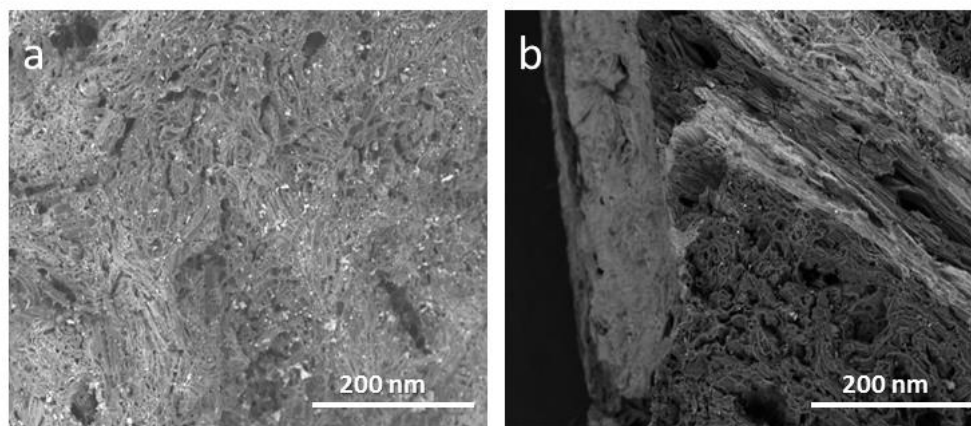

Figure 3: SEM images of the fresh Ru-STA-AC sample (a), and the same catalytic material after reaction (b).

The specific activities of catalysts were determined for two model test reactions (i.e. isomerization of 3,3-dimethyl-1-butene and cyclohexane dehydrogenation) and gathered in Table 1. Cyclohexane dehydrogenation is known to be catalysed only by the metallic phase and to be insensitive to the particle structure [31]. Catalytic dehydrogenation of cyclohexane produces only benzene as product, while the 3,3-dimethyl-1-butene isomerization involves only Bronsted acidic sites and occurs through a pure protonic mechanism, leading to two reaction products, i.e. 2,3-dimethyl-2-butene and 2,3-dimethyl-1-butene [30]. For both bifunctional catalysts, Ru-STA-AC and Ru-TPA-AC, the initial catalytic activities, measured by dehydrogenation test, are in the same range of magnitude (0.2 mol/h·g_{metal}) because these two materials content the same metallic contribution. This similitude can be expected, since the percentage of ruthenium

impregnated (2 wt%) is the same, and the average Ru particle size determined by TEM are into the same range (< 4 nm). However, considering the acidic contribution, the activities for the isomerization test reaction evidence some significant differences between both catalysts. Effectively, the catalyst prepared with STA exposes an increased number of acidic centres or acidic sites of higher strength (70 mmol/h·$g_{catalyst}$) in comparison with TPA derivative (45 mmol/h·$g_{catalyst}$). This fact may be due to two reasons: the higher number of protons in STA structure (4 H$^+$ in STA vs 3 H$^+$ in TPA) and the higher acidity of STA. The higher acidity may be caused by the less electron density in STA surface than TPA ones. So, Izumi et al. [32] studied the properties of these POM and the better activities of STA in acid catalysis were attributed to the greater softness of the STA anion (STA conjugated base), and therefore the minor electronic density over surface which allows an enhanced proton mobility [33].

Table 1: Results of initial catalytic activities for both test reactions

Catalyst	Dehydr. Activity [a] (mol/h·g_{metal})	Isom. Activity [b] (mmol/h·$g_{catalyst}$)
Ru-STA-AC	0.15	70
Ru-TPA-AC	0.20	45

a: Initial activity for dehydrogenation reaction test
b: Initial activity for isomerization reaction test

3.2 Catalytic reaction studies

Before the catalytic tests, the solvent which will be used should be selected reasonably. Water is one of desirable and green option, but unfortunately, as it is mentioned previously, POMs are easily dissolved in aqueous media. In previous reports where these polyoxometalates are applied, around 50-60% of dissolved POMs in aqueous media were detected by ICP-OES [27]. Ethanol is considered as another green solvent which could be a substitute of water in some cases, so a mixture of ethanol:water (9:1) was chosen as solvent in this study. Some polyols, such as sorbitol, are not soluble in ethanol and it is for that water is a tenth part of reaction media.

The possible leaching of metals (mainly W and Ru) was studied by ICP-OES analysis of the reaction medium after 5 h reaction at 413 K, and the results presented in Table 2 evidence an important leaching of POM ($\approx$ 40%). Unfortunately, the high solubility of POMs in water makes the little quantity of water used as solvent (only 1 tenth part) to be sufficient to dissolve almost the half part of supported POM. Perhaps the bigger crystallites of POM, observed by SEM (Figure 3a), could suffer an easily leaching to reaction media. Contrarily, only around 0.2-0.3 % of Ru total amount supported over carbonaceous material lixiviates, hence we can assume that the leaching of Ru nanoparticles is negligible.

Table 2: Results of metal leaching after reaction.

Catalyst	POM leaching (%)	Ru leaching (%)
Ru-STA-AC	37	0.15
Ru-AC + STA-AC	41	0.37

Furthermore, knowing that sugars could suffer thermal decomposition, low temperatures have to be used in the catalytic reaction. We assume that 413 K is an adequate temperature since in previous reports this temperature has conducted to good results in sugars transformations [27]. Then, a set of experiments without catalyst, under these selected soft reaction conditions (413 K and 30 bar H_2) and using three different reactants (sucrose, glucose and fructose) in ethanol/water (9:1) mixture as solvent, have been performed. So, these three blank reactions produce less than 10% of conversions and 3% of yields in targeted products after 6 h of reaction. Also the reactor was loaded with reactant (sucrose, glucose and fructose) and the bare carbon support (AC), and similar results have been achieved, therefore the thermal decomposition of sugars with or without carbon support doesn't occur and the catalytic activity displayed during blank experiments is negligible. Taking into account these results, the same conditions have been selected to evaluate the catalytic materials.
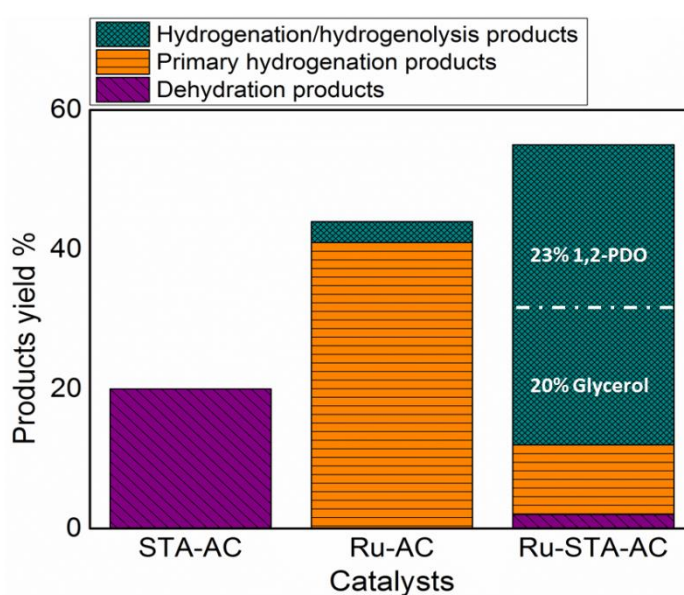

Figure 4: Catalytic activity of monofunctional (acid or metallic) and bifunctional catalysts at 5 h of reaction and using sucrose as reactant.

In the first set of experiments, monofunctional (STA-AC and Ru-AC) and bifunctional (Ru-STA-AC) catalysts were tested using sucrose as reactant. Figure 4 shows the obtained product yields. Firstly it should be mentioned that the acid monofunctional material (STA-AC) doesn't catalyse the interest reaction and 1,2-propanediol, produced by hydrogenation/hydrogenolysis, is not detected. However, catalytic conversion of sucrose is significant since the reactant is dehydrated to 5-hydroxymethyl furfural (step 3 in Scheme 1). This result suggests that a metallic contribution is compulsory for achieving sucrose hydrogenation/hydrogenolysis. This is reasonable because the synthesis of sorbitol/mannitol from glucose or fructose (see Scheme 1, step 4 or 5) is a hydrogenation reaction, which is catalysed by metals such as ruthenium [15,34]. Therefore, the catalysts with Ru metallic contribution (monofunctional (Ru-AC) and bifunctional (Ru-STA-AC)) should be more efficient for this transformation. Using the same soft reaction conditions, a high production of sorbitol and mannitol mixture is reached using the monofunctional catalyst (Ru-AC), since mainly hydrogenation reactions take place (steps 4 and 5 of Scheme 1). Other relevant question is the production of glucose and fructose from sucrose, since mannitol and sorbitol are derived products of these monosaccharides. As it is mentioned above, for hydrolysis of sucrose into fructose and glucose an acid contribution is needed. Therefore, Ru-AC solid presents also some acidity, perhaps derived of both the activated carbon surface groups or from the Ru nanoparticles itself. Interestingly, when the catalyst contains also POM (Ru-STA-AC), the reaction goes forwards glycerol and 1,2 PDO synthesis (pathways 6, 7, 8 or 9 of Scheme 1). However, the exact pathway followed during the reaction remains unclear, this issue will be examined later in this contribution. In conclusion, a bifunctional catalyst is necessary using these reaction conditions to transform sucrose

into 1,2 PDO. Also, another relevant premise of this experiment can be extracted seeing that the main products are the hydrogenation/hydrogenolysis compounds, which means that the metallic contribution (Ru nanoparticles) dominates over acidic contribution (POM), since the reaction follows the paths 4/5 or 6/7 versus step 3 of Scheme 1. Taking into account these preliminary results, the next set of experiments (Table 3) were carried out using bifunctional Ru-STA-AC catalyst, and aimed at determining if obtained PDO comes from fructose or from glucose.

Given that the interest product (PDO) can be obtained following two different paths (one via intermediate compounds, i.e. sorbitol/mannitol then glycerol (steps 6, 7 and 8 Scheme 1), and the second directly from fructose (step 9 Scheme 1)), the results showed in Table 3 reveal that when the reaction starts from glucose (row 1) mainly sorbitol and E-glucose were detected, while mainly glycerol and 1,2-PDO were identified when fructose is the reactant (row 2). In the first case, it seems that the glucose is hydrogenated to sorbitol and subsequent reactions are halted. In order to find an explanation for this situation, sorbitol and the same bifunctional catalyst (Ru-STA-AC) were tested (row 3), but the same behaviour is observed, with any glycerol and 1,2-PDO detected and a remarkably low sorbitol conversion (around 30%). So, in order to study the possible adsorption of the polyol onto or into the activated carbon, the catalyst (Ru-STA-AC) recovered after reaction was washed with heat water and the washing liquids analysed by HPLC. The results confirm that the sorbitol molecules are adsorbed over AC, probably due to the porous structure of this carbon support.

Table 3: Conversion, products yield and carbon balances after 5 h reaction time using bifunctional Ru-STA-AC catalyst and different reactants.

	Reactant	Conv. (%)	Yield %				Carbon balance (%)
			E-glucose/E-fructose	Sorbitol/Mannitol	Glycerol	1,2-PDO	
1	Glucose	82	39	31	2	3	97
2	Fructose	93	3	0.6	41	48	98
3	Sorbitol	28	-	-	-	-	72
4	Mannitol	40	-	-	-	-	60
5	Glycerol	5	-	-	-	-	95

Seeing that there are many reported studies about the synthesis of 1,2-PDO from sorbitol using monofunctional ruthenium catalysts [35, 36, 37], we carried out another experiment using sorbitol and ruthenium catalyst (Ru-AC) under our reaction conditions. The sorbitol conversion obtained after 5h reaction was less than 10% and any yield of interest products was detected, so we assume that glycerol and 1,2-PDO with a monofunctional metallic catalyst (Ru-AC) can not be synthetized. The important difference between the reported studies and this one is the value of the reaction temperature. Indeed, it seems that with high temperature (493 K) the hydrogenation/hydrogenolysis compounds can be obtained only with metallic contribution, but when using low reaction temperature (413 K) the presence of acidic sites over catalyst surface is compulsory.

Finally, using the Ru-STA-AC catalyst, targeted products yields are higher where fructose is used as reactant, particularly the PDO yield is close to 50% (Table 3, row 2). This increase of PDO yield, in comparison with the case of sucrose used as reactant (Figure 4), is expected as half part of sucrose converted to glucose is then not transformed to PDO (row 1 of Table 3). Following the evidences extracted from these results, it is possible to assume that the best compound for yielding PDO is the fructose, and consequently the next set of catalytic experiments will be based on a comparison of fructose transformation over the monofunctional and the bifunctional catalysts.

But first of all, the understanding of reaction paths is going to be addressed. Then, using sorbitol or mannitol as reactants (row 3 and row 4 in Table 3), similar catalytic results are observed in both cases. As mentioned above, the consumption of sorbitol during the reaction can be explained through sorbitol adsorption over activated carbon, thus the same explanation will justify the mannitol conversion. These similar behaviours seem to be in agreement with obtained carbon balances, since the percentages of conversion (40%) is value needed to complete the 100% of carbon balance. However the results obtained with glycerol as reactant (row 5 of Table 3) were not the expected ones, since in a majority of reported articles the glycerol appears such as intermediate compound and evolves through hydrogenolysis reaction to 1,2-PDO [38, 39]. Therefore, the predictable behaviour would be an appearance of glycerol during the first hours of reaction and later its consumption at the same time that 1,2-PDO is formed. According to the row 5 of Table 3, a different situation occurs since none of glycerol reacts to produce 1,2-PDO under the selected experimental conditions. When glycerol is synthetized, seems to be that it doesn't readsorb over catalyst surface to start the catalytic heterogeneous transformation to PDO. In the same line, the evolution of fructose consumption and reaction products displayed in Figure 5 during 5 h of reaction

shows that both glycerol and 1,2-PDO are produced independently. So, evidently the glycerol isn't an intermediate compound during the transformation of fructose to 1,2-PDO. Then, from the results of these two experiments (Table 3-row 5 and Figure 5), we can conclude that when glycerol is synthetized and desorbed, it doesn't adsorb again over catalytic material to be transformed according to step 8 of Scheme 1. Consequently, the 1,2-PDO production is limited by glycerol production due to the non-reactive character of the synthetized glycerol. Another relevant aspect observed in Figure 5 is that mannitol doesn't appear throughout the catalytic transformation of fructose, which means that synthesis of glycerol and 1,2-PDO seem occur via direct pathway from fructose (steps 6 and 9 of Scheme 1). Moreover, this behaviour is in agreement with results showed in Table 3-row 3, since if mannitol could be produced during the sorbitol transformation reaction, it shouldn't produce glycerol or 1,2-PDO. Thus, a direct pathway from fructose to glycerol and PDO, following only the steps 6 and 9 of Scheme 1, can be concluded in agreement with other reported articles [19].
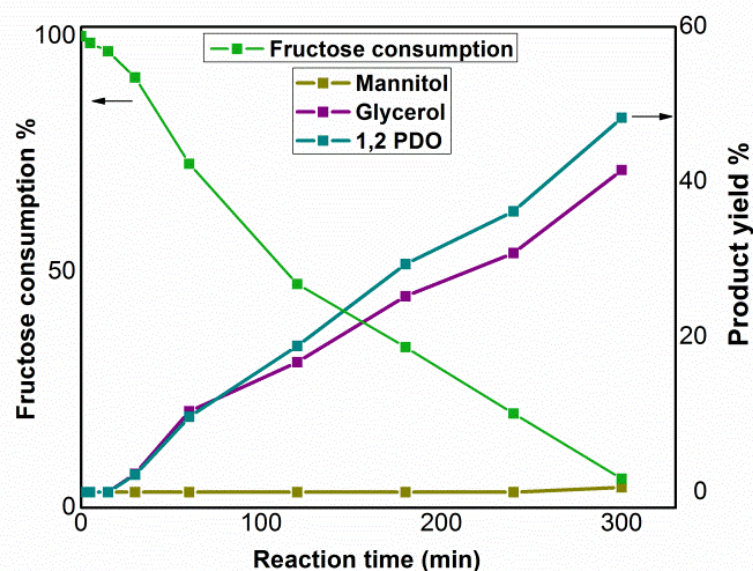

Figure 5: Evolution of fructose consumption and product yields (%) during 5 h of reaction using Ru-STA-AC, at 413 K and with EtOH/H_2O as solvent.

Due to the clear advantages presented by fructose as reactant (direct path and high PDO yield), the catalytic study of the fructose transformation was intensified firstly evaluating the catalytic activities of the different materials (monofunctional or bifunctional), and secondly analysing what happens when the two catalyst functionalities (acid and metal) are provided by a physical mixture of two catalytic materials each one with one active phase. Figure 6 shows that the best yield of targeted products are reached using bifunctional catalyst (Ru-STA-AC) in comparison to monofunctional material (Ru-AC). Particularly, the monofunctional metal catalyst produces poor fructose conversion and PDO yield; whereas, as already mentioned previously, the bifunctional material leads to high PDO yield and selectivity (48% and 50% respectively). These results are comparable with those of the scientific literature. So, Liu et al. [19] already mentioned that 55% of PDO selectivity can be achieved at 453 K from glucose transformation over alumina supported copper and tungsten oxide catalysts. Also, with the same temperature of reaction, Hirano et al. [21] reported the transformation of glucose to propylene glycol (1,2-PDO) and ethylene glycol as principal products with yields of 13% and 21%, respectively, on Ru/C catalysts combined with ZnO. In these two studies, the reaction temperature is higher than in our case, probably because glucose in comparison with fructose needs high temperatures to be converted into PDO. In fact, as it was reported in Table 3, at 413 K with the Ru-STA-AC catalyst, glucose only produces sorbitol.

Furthermore, Figure 6 reveals that when the two catalytic functionalities (metallic and acidic) are physically separated (physical mixture of Ru-AC and STA-AC samples) catalytic activity is significantly decreased in comparison with Ru-STA-AC catalyst, and the yield to 1,2-PDO is also diminished. This means that the arrangement of both

catalytic functionalities, supported over activated carbon, plays a crucial role in this catalytic transformation. Thus, the presence of Ru nanoparticles and POM crystallites in near nanometric proximity is determining on the catalytic performance. Provably this surface nanometric arrangement acts favouring the interactions of intermediate species generated over the metallic sites improving the action of the acidic centres of POM. Thanks to the inert property of AC, this essential arrangement among both active phases is accomplished because this support doesn't contribute to strong interactions, neither with Ru particles nor with POM crystallites. In this way the interactions between Ru nanoparticles and POM are favoured, achieving these nanometric arrangements, where the catalytic action is maximized.

On the SEM images of fresh Ru-STA-AC, the presence of POM crystallites of large sizes was clearly observable (Fig. 3a). Contrarily on the SEM images of the used catalyst (Fig. 3b) most of the larger POM particles of polyoxometalate disappeared, the smaller POM particles, less observable on the SEM images, were however detectable by the electron dispersed X-ray analysis. Evidently, during reaction there is some quantity of dissolved POM acting as homogeneous catalyst. Nevertheless the amount of lixiviated polyoxometalate should be similar than in the catalytic experiment performed with physical mixture (Ru-AC + STA-AC), but the advantages obtained with the bifunctional catalyst (Ru-STA-AC) remain remarkable (Figure 6). This means that the catalytic activity of a mixture of dissolved POM and Ru-AC catalyst is not sufficiently active to transform the fructose into interest compounds. In order to confirm this point, another experiment was performed using the Ru-AC catalyst with an amount of STA previously dissolved in the reaction media equivalent to that incorporated in the STA-AC sample. This experiment denoted as Ru-AC+STA in Figure 6 reveals again that selectivity to 1,2-PDO required the neighbouring presence of Ru and POM

nanoparticles. Thus, it is clear that nanometric proximity between Ru nanoparticles and smaller POM crystallites (acidic phase) is the responsible of the higher yields achieved with the bifunctional Ru-STA-AC catalyst for the fructose transformation into 1,2-PDO. Finally, in order to verify the improved catalytic performance in the fructose hydrogenation/hydrogenolysis, the second bifunctional catalyst prepared from TPA (Ru-TPA-AC) was evaluated. This sample was also a suitable catalyst for fructose transformation in terms of catalytic conversion and of yield to 1,2-PDO (Figure 6). However, the catalytic performances of Ru-TPA-AC catalyst are lower compared to those of Ru-STA-AC, which can be due to the smaller acidic activity achieved with the catalyst prepared using TPA according to the characterization results reported in Table 1 (36 mmol/h·$g_{catalyst}$ versus 63 mmol/h·$g_{catalyst}$). This difference in acidity, as discussed above, cannot be only due to the various density of protons of the two studied POMs (4 in the case of STA ($H_4[W_{12}SiO_{40}]$) and 3 for TPA ($H_3PW_{12}O_{40}$)), so another fact such as electron density in POM surface could modify the acid strength. Moreover, the TPA catalyst also produces poor carbon balance in comparison to STA ones. Probably this polioxometalate leads the reaction to production of undesirable products including humic acids which deactivate the acid solid [25]. Also, the selectivity to interest products presented by TPA sample is slightly different vs STA ones, as on the former the mannitol formation is detected. As it is showed in Table 1, the STA catalyst presents higher acidity than the TPA ones, therefore the ratio metallic/acidity functionality is not the same in both bifunctional materials. Probably, the lower acidity in Ru-TPA-AC causes that the metallic contribution gains importance versus acid contribution and then the fructose can follow two different pathways: the direct transformation to PDO (step 9 of scheme 1) and the fructose hydrogenation to mannitol (step 5 of scheme 1).
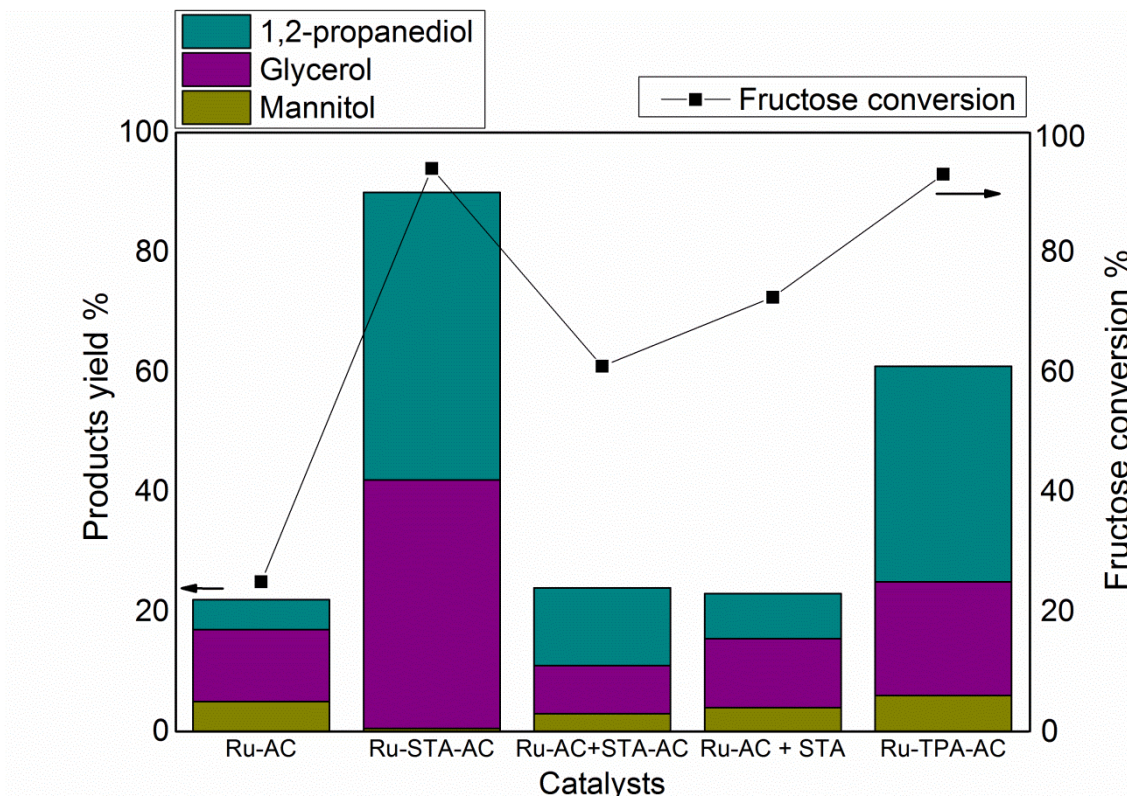
Figure 6: Comparison of the catalytic performances of monofunctional, bifunctional (two POMs: STA and TPA) and physical mixture catalysts with the same reaction conditions and using fructose as reactant after 5 h at 413 K and with EtOH/H_2O as solvent.

However, the improved catalyst (Ru-STA-AC) suffers leaching of POM and probably a deactivation. In order to verify this catalytic activity loss, a used catalyst was tested under the same reaction conditions. The Table 4 presents the results obtained with used catalyst (reuse), where it is possible to see that the loss of activity in the second run expressed as percentage (43%) almost corresponds with the value of POM leaching in the first run (40%).

Table 4. Catalytic performance during the recycling use for the fructose transformation after 5h at 413 K and with EtOH/H$_2$O as solvent.

Catalyst	Conversion (%)	PDO Yield (%)	Glycerol yield (%)	Sum of yields (%)	Loss activity (%)
Ru-STA-AC	93	48	41	89	0
Reuse	55	20	30	50	43

4. Conclusions

To summarize, monofunctional and bifunctional catalysts formed by ruthenium nanoparticles or/and POM supported over activated carbon have been studied in the hydrogenation/hydrogenolysis of sugars at 413 K. From the catalytic performances and characterization results described in this paper, some conclusions can be established. Using monofunctional catalysts, STA-AC or Ru-AC, none of interest compounds are reached in the catalytic transformation of sucrose. Particularly, with the second one, in disagreement with reported bibliography, only hydrogenation compound (sorbitol or mannitol) can be distinguished. On the contrary, the use of a new bifunctional material synthetized with 15 wt % of POM and 2 wt % of Ru supported on activated carbon (Ru-STA-AC) leads to high yield and selectivity of interest compound (1,2-PDO). Thus combining both functionalities (acidic and metallic) is compulsory for the sucrose transformation to 1,2-PDO at low reaction temperature. Due to the low reactivity of glucose under the studied conditions, the best results, in terms of catalytic activity, are achieved starting from fructose as reactant and with Ru-STA-AC catalyst leading to 48% of yield and 50% of selectivity in 1,2-PDO, evidently overcoming the sucrose

transformation results. Interestingly, using fructose as reactant, other relevant conclusion can be extracted, since when the catalytic reaction is carried out with a physical mixture of two monofunctional catalysts (Ru-AC + STA-AC), an evident decrease of conversion and PDO yield is observed. Therefore, a nanometric arrangement between active species is necessary, and these interactions are reached thanks to the activated carbon properties. The inert character of this carbonaceous material provokes weak interactions with polyoxometalates, thus favoring stronger interactions between the two actives phases. A relevant conclusion is that, as we would believe, the type of carbon support used in the new catalytic material synthesis plays an important role since the catalytic activity is strongly dependent on the interactions among POM crystallites and Ru nanoparticles. Finally, from a detailed study of the reaction pathways, we postulate that (i) fructose transformation follows a direct route to produce PDO due to the absence of mannitol as intermediary product in the course of reaction, (ii) glycerol is not an intermediate compound of the PDO synthesis since glycerol and PDO appear simultaneously, and (iii) synthesis of PDO is also limited by glycerol production since glycerol generated in reaction media cannot evolve further toward PDO.

References

[1] M. Besson, P. Gallezot, C. Pinel, Chem. Rev. 114 (2014) 1827−1870.

[2] J. Song, H. Fan, J. Ma, B. Han, Green Chem. 15 (2013) 2619–2635.

[3] D.M. Alonso, J.Q. Bond, J.A. Dumesic, Green Chem. 12 (2010) 1493–1513.

[4] M.J. Climent, A. Corma, S. Iborra, Green Chem. 16 (2014) 516–547.

[5] Z. Xue, M.-G. Ma, Z. Li, T. Mu, RSC Adv. 6 (2016) 98874–98892.

[6] I. Bodachivskyi, U. Kuzhiumparambil, D.B.G. Williams, ChemSusChem. 11 (2017) 642–660.

[7] R. Palkovits, K. Tajvidi, A.M. Ruppert, J. Procelewska, Chem. Commun. 47 (2011) 576–578.

[8] J.N. Chheda, G.W. Huber, J.A. Dumesic, Liquid-phase catalytic processing of biomass-derived oxygenated hydrocarbons to fuels and chemicals, Angew. Chemie - Int. Ed. 46 (2007) 7164-7183.

[9] J.C. Serrano-Ruiz, R. Luque, A. Sepúlveda-Escribano, Transformations of biomass-derived platform molecules: From high added-value chemicals to fuels via aqueous-phase processing, Chem. Soc. Rev. 40 (2011) 5266-5281.

[10] X. Hu, L. Wu, Y. Wang, Y. Song, D. Mourant, R. Gunawan, M. Gholizadeh, C.Z. Li, Bioresour. Technol. 133 (2013) 469–474.

[11] X. Hu, S. Wang, R.J.M. Westerhof, L. Wu, Y. Song, D. Dong, C.Z. Li, Fuel. 141 (2015) 56–63.

[12] Y. Liu, C. Luo, H. Liu, Angew. Chemie - Int. Ed. 51 (2012) 3249–3253.

[13] M. Almohalla, I. Rodríguez-Ramos, L.S. Ribeiro, J.J.M. Órfão, M.F.R. Pereira, A. Guerrero-Ruiz, Catal. Today. 301 (2018) 65–71.

[14] A.M. Ruppert, K. Weinberg, R. Palkovits, Angew. Chemie, 51 (2012) 2564–2601.

[15] C. Liu, C. Zhang, K. Liu, Y. Wang, G. Fan, S. Sun, J. Xu, Y. Zhu, Y. Li, Biomass and Bioenergy. 72 (2015) 189–199.

[16] P.A. Lazaridis, S. Karakoulia, A. Delimitis, S.M. Coman, V.I. Parvulescu, K.S. Triantafyllidis, Catal. Today. 257 (2015) 281–290.

[17] P.A. Lazaridis, S.A. Karakoulia, C. Teodorescu, N. Apostol, D. Macovei, A. Panteli, A. Delimitis, S.M. Coman, V.I. Parvulescu, K.S. Triantafyllidis, Appl. Catal. B Environ. 214 (2017) 1–14.

[18] J.M.A.R. Almeida, L. Da Vià, P. Demma Carà, Y. Carvalho, P.N. Romano, J.A.O. Peña, L. Smith, E.F. Sousa-Aguiar, J.A. Lopez-Sanchez, Catal. Today. 279 (2017) 187–193.

[19] C. Liu, C. Zhang, S. Hao, S. Sun, K. Liu, J. Xu, Y. Zhu, Y. Li, Catal. Today. 261 (2016) 116–127.

[20] C. Liu, C. Zhang, S. Sun, K. Liu, S. Hao, J. Xu, Y. Zhu, Y. Li, ACS Catal. 5 (2015) 4612–4623.

[21] Y. Hirano, K. Sagata, Y. Kita, Appl. Catal. A Gen. 502 (2015) 1–7.

[22] W. Deng, Q. Zhang, Y. Wang, Dalt. Trans. 41 (2012) 9817–9831.

[23] J. Chen, S. Wang, J. Huang, L. Chen, L. Ma, X. Huang, ChemSusChem. 6 (2013) 1545–1555.

[24] L.R. Pizzio, C. V. Cáceres, M.N. Blanco, Appl. Catal. A Gen. 167 (1998) 283–294.

[25] M. Haruta, Chem. Rec. 3 (2003) 75–87.

[26] M. Ghaedi, S. Heidarpour, S. Nasiri Kokhdan, R. Sahraie, A. Daneshfar, B. Brazesh, Powder Technol. 228 (2012) 18–25.

[27] N. García Bosch, B. Bachiller-Baeza, I. Rodriguez-Ramos, A. Guerrero-Ruiz, ChemCatChem. 10 (2018) 3746– 3753.

[28] M.A. Schwegler, P. Vinke, M. van der Eijk, H. van Bekkum, Appl. Catal. A, Gen. 80 (1992) 41–57.

[29] J. Alcañiz-Monge, G. Trautwein, S. Parres-Esclapez, J.A. Maciá-Agulló, Microporous Mesoporous Mater. 115 (2008) 440–446.

[30] S. N. Delgado, D. Yap, L. Vivier, C. Especel, Journal of Molecular Catalysis A: Chemical 367 (2013) 89– 98.

[31] D. Messou, L. Vivier, C. Especel, Energy Conversion and Management. 127 (2016) 55–65.

[32] Y. Izumi, K. Matsuo, K. Urabe, Journal of Molecular Catalysis, 18 (1983) 299 - 314.

[33] A.B. Yaroslavtsev, Russian Chemical Reviews, 63 (1994) 429-435.

[34] J. Zhang, J.B. Li, S. Bin Wu, Y. Liu, Ind. Eng. Chem. Res. 52 (2013) 11799– 11815.

[35] I. Murillo Leo, M. López Granados, J.L.G. Fierro, R. Mariscal, Appl. Catal. B Environ. 185 (2016) 141–149.

[36] J.H. Zhou, M.G. Zhang, L. Zhao, P. Li, X.G. Zhou, W.K. Yuan, Catal. Today. 147 (2009) 225–229.

[37] L. Zhao, J.H. Zhou, Z.J. Sui, X.G. Zhou, Chem. Eng. Sci. 65 (2010) 30–35.

[38] J. N. Chheda, G. W. Huber, J. A. Dumesic, Angew. Chemie. 46 (2007) 7164–7183.

[39] W. Yin, Z. Tang, R. H. Venderbosch, Z. Zhang, C. Cannilla, G. Bonura, F. Frusteri, H. J. Heeres, ACS Catal. 6 (2016) 4411–4422.